

Magnetic frustration and the onset of magnetic order in the pyrochlore  
iridate  $\text{Nd}_2\text{Ir}_2\text{O}_7$

S. M. Disseler<sup>1</sup>, Chetan Dhital<sup>1</sup>, T. C. Hogan<sup>1</sup>, A. Amato<sup>2</sup>, S. Giblin<sup>3</sup>, Clarina de la Cruz<sup>4</sup>,  
S. D. Wilson<sup>1</sup>, and M. J. Graf<sup>1\*</sup>

<sup>1</sup> Department of Physics, Boston College, Chestnut Hill, MA 02467 USA

<sup>2</sup> Paul Scherrer Institute, CH 5232 Villigen PSI, Switzerland

<sup>3</sup> Rutherford Appleton Laboratory, Didcot, Oxfordshire OX11 0QX, UK

<sup>4</sup> Neutron Scattering Science Division, Oak Ridge National Laboratory, Oak Ridge, TN  
37831-6393, USA

Abstract

We report a combined  $\mu\text{SR}$ , bulk magnetization, and transport study of the electronic properties of  $\text{Nd}_2\text{Ir}_2\text{O}_7$ . We observe the onset of strongly hysteretic behavior in the temperature dependent magnetization below 120 K, and an abrupt increase in the temperature dependent resistivity below 8 K. Zero field muon spin relaxation measurements show that the hysteretic magnetization is driven by a transition to a magnetically disordered state, and that below 8 K magnetic order sets in, as evidenced by the onset of heavily damped spontaneous muon precession. Our measurements point toward the formation of a complex magnetic ground state and the absence of a true metal-to-insulator phase transition in this material.

Pyrochlore structures with  $A_2B_2O_7$  stoichiometry have attracted a great deal of attention in recent years [1]. The crystalline structure consists of two interpenetrating networks of corner-sharing tetrahedra on which the A and B ions reside. The geometric structure is known to frustrate magnetic order, which can produce novel, highly degenerate ground states such as spin-ice/spin-liquid states [2]. In many such systems, correlations allow for the system to relieve this frustration via lattice distortions and metal-insulator transitions. The pyrochlore iridate family  $A_2Ir_2O_7$  (A = Y or lanthanide element) is predicted to exhibit a wide range of novel behaviors including topologically nontrivial phases depending on the correlation strength [3 - 5]. Earlier work has suggested that the correlation strength can be tuned by choice of the lattice A-site: with increasing ionic radius the system crosses over from an insulating ground state (e.g., A = Y or Eu) to a metallic ground state (A = Pr). A metal-insulator (MI) transition is reported at temperatures  $T_{MI}$  ranging from 150 K for  $Y_2Ir_2O_7$  [5, 6] to 37 K for  $Nd_2Ir_2O_7$  [7], indicating that  $T_{MI}$  decreases with increasing ionic radius. Additionally, weak magnetic order, presumed to be antiferromagnetic due to the lack of a net moment, was inferred from anomalies in the temperature dependent magnetization for those members of this family that exhibit an insulating ground state [6, 7]. Recent muon spin relaxation/rotation ( $\mu$ SR) measurements have confirmed this overall picture: the onset of long range magnetic order observed via spontaneous muon precession in zero magnetic field was observed in insulating  $Eu_2Ir_2O_7$ [9],  $Y_2Ir_2O_7$  [10] and  $Yb_2Ir_2O_7$ [10] in the vicinity of the magnetization anomaly whereas metallic  $Pr_2Ir_2O_7$  shows no signs of long-range order down to 0.3 K [11]. As  $Eu^{3+}$  and  $Y^{3+}$  are non-magnetic, the order must originate from the Ir moments where the size of the  $Ir^{4+}$  moment is estimated to be roughly  $1 \mu_B$  and consistent with  $J_{eff} = 1/2$ .

Within the iridate pyrochlores,  $Nd_2Ir_2O_7$  is of particular interest to study because it has a relatively large ionic radius and also the lowest reported  $T_{MI}$ , suggesting that it is at the boundary of metallic and insulating behavior and hence potentially susceptible to instabilities. The precarious nature of the insulating state is evidenced by the variability in previously reported properties: in Ref. 5 the sample was clearly metallic at all temperatures, while in Ref. 7 an MI transition was observed at 37 K. Studies of the resistivity under pressure [12] show that a small upturn below 20 K in the temperature

dependent resistivity at low pressures (2 GPa), which was interpreted as the onset of the MI transition, was suppressed by applied pressure of 10 GPa. At higher pressures, a small resistive anomaly was observed near  $T = 3.3$  K which the authors associate with the onset of magnetic order via an RKKY interaction facilitated by the suppression of the MI transition. The magnetic order was presumed to be ferromagnetic based on the detailed magnetic response of the resistivity, with a 2-in/2-out structure of the  $\text{Nd}^{3+}$  ( $J = 9/2$ ) moments. Recent neutron scattering measurements, however, suggest that magnetic order occurs at ambient pressure with long-range magnetic order (LRMO) of the  $\text{Ir}^{4+}$  moments setting in below 15 K [14] in a structure consistent with an all-in/all-out arrangement. Thus fundamental questions regarding the nature of the low-temperature ground state of  $\text{Nd}_2\text{Ir}_2\text{O}_7$  are at present unresolved.

In this work we present magnetization, electrical resistivity, neutron diffraction, and muon spin relaxation/rotation data for polycrystalline samples of  $\text{Nd}_2\text{Ir}_2\text{O}_7$ . This is the first comprehensive study of this material using both bulk and local probes on the same samples. We find the onset of a disordered magnetic state at 120 K, as observed for other members of the  $\text{A}_2\text{Ir}_2\text{O}_7$  [6] and presumed to be associated with the  $\text{Ir}^{4+}$  sublattice, with no evidence for a metal-insulator transition in this system at any temperature. Below 8 K, we observe the onset of long-range magnetic order, also associated with the  $\text{Ir}^{4+}$  sublattice as evidenced by the onset of spontaneous zero field muon precession.

Polycrystalline samples of  $\text{Nd}_2\text{Ir}_2\text{O}_7$  were synthesized by reacting stoichiometric amounts of  $\text{Nd}_2\text{O}_3$  (99.99%) and  $\text{IrO}_2$  (99.9%). Powders were pelletized using an isostatic cold press and reacted at temperatures between 900 C to 1125 C over a period of six days with several intermediate grindings. The samples were determined to be phase-pure with the exception of two minor impurity phases of  $\text{IrO}_2$  and  $\text{Nd}_2\text{O}_3$  each comprising less than 1% of the total volume fraction. Neutron experiments were performed on the HB-2A powder diffractometer at the High Flux Isotope Reactor at Oak Ridge National Lab. A  $\lambda_i = 1.5385$  Å was used with a Ge(115) monochromator and 12'-31'-60' collimation, and data were refined using the FullProf software package. Magnetization measurements were performed in an Oxford MagLab dc-extraction magnetometer and the electrical resistivity was measured using standard AC four-probe techniques in a gas flow cryostat with 9T magnet. Magnetic fields up to 9 T were applied parallel to the current, and the

excitation level was varied at several temperatures to ensure no self-heating occurred. Muon spin relaxation ( $\mu$ SR) measurements were carried out over the temperature range  $1.6 \text{ K} < T < 150 \text{ K}$  on the EMU spectrometer at the ISIS pulsed beam facility at the Rutherford Appleton Laboratories, and the GPS spectrometer on the  $\pi$ M3 continuous beamline at Paul Scherrer Institute (PSI). Powder samples were studied at ISIS in a silver holder with a Mylar window, and the small contribution (10%) of muons stopping in the silver was independently measured and subtracted from the data. Powder samples at PSI were sealed in metalized Mylar packets, with no background contribution.

The temperature dependent static susceptibility  $\chi(T)=M/H$  of polycrystalline  $\text{Nd}_2\text{Ir}_2\text{O}_7$  was measured from 250 K to 1.8 K in samples under a field of 1000 Oe under both zero field cooled (ZFC) and field cooled (FC) conditions, and the results are shown in Fig. 1a. Under ZFC conditions, we observe a small peak in  $\text{Nd}_2\text{Ir}_2\text{O}_7$  at 105 K, while under FC conditions we see a sharp increase at  $T = 120 \text{ K}$ . This behavior is similar to that observed for other members of the  $\text{A}_2\text{Ir}_2\text{O}_7$  family and occurs at a comparable temperature [6]. It is associated with the onset of magnetism in the  $\text{Ir}^{4+}$  sublattice, as it occurs when the A-site species is either magnetic or non-magnetic. The anomaly is typically linked to a MI transition, which occurs at comparable temperatures [5 - 7] for several members of the  $\text{A}_2\text{Ir}_2\text{O}_7$  family. The onset temperature of the magnetic anomaly from these magnetization measurements however is considerably higher than the value of  $T_{MI} = 37 \text{ K}$  extracted from earlier resistivity measurements in Ref. 7. Upon continued cooling below 100 K there is a significant difference between the FC and ZFC behavior until 8 K, below which the ZFC and FC curves converge with negative curvature  $d^2M/dT^2$ .

Turning to field dependent resistivity measurements on the same sample, the temperature dependent resistivity of  $\text{Nd}_2\text{Ir}_2\text{O}_7$  is shown in Fig. 1b. A decrease in the resistivity is observed below room temperature and reaches a broad minimum at  $T \sim 65 \text{ K}$ . Between 65 K and 8 K, there is a very weak increase in the resistivity; however below 8 K there is a second slope-change followed by a clear tendency towards saturation. An applied magnetic field of 9 T in the region above 8 K has very little effect on the resistance, in contrast to the large negative magnetoresistance that is observed at lower temperatures. To verify this behavior, samples from two different batches were measured,

including one sample before and after a 24 hour anneal in an oxygen environment, and in all cases the data were the same.

In Fig. 2, we show the magnetic field dependence at  $T = 1.8$  K of both the magnetization and resistivity. The  $J = 9/2$  state is known to split into 5 Kramers doublets in the crystal field of the magnetic ion, assuming a trigonal symmetry [13]. Therefore, a nonlinear least-squares fit of a Brillouin function with  $J_{eff} = 1/2$  was used to describe the data. The fit is shown as the dashed curve in Fig. 2, corresponding to paramagnetic moments with  $J_{eff} = 1/2$  and an effective moment  $\mu_{eff} = 1.3 \pm 0.1 \mu_B$ . This  $\mu_{eff}$  is larger than the maximum estimated size of the  $\text{Ir}^{4+}$  moment but smaller than the free  $\text{Nd}^{3+}$  moment. From this, we conclude that the Nd moments remain paramagnetic down to at least 1.8 K whereas the  $\text{Ir}^{4+}$  moments undergo a magnetic transition at 120 K.

As an initial probe of the correlated  $\text{Ir}^{4+}$  spin order, elastic neutron scattering measurements were performed. The resulting neutron diffraction patterns were refined using the Fd-3m cubic space group, and the lattice parameters were determined to be  $a = 10.3588(4)$  Å at 4 K and  $a = 10.3647(9)$  Å at 200 K. However, our measurements did not show any evidence of long-range magnetic order down to 4 K with the upper bound of an ordered moment conservatively estimated to be  $0.5 \mu_B$ .

In order to explore the magnetic order further,  $\mu\text{SR}$  measurements were performed on two spectrometers with complementary resolutions/sensitivities to both fast relaxation processes (GPS at PSI) and slow relaxation processes (EMU at ISIS). In combining these measurements, we obtain a picture of both static and fluctuating magnetic fields throughout the bulk of the sample over a broad frequency domain. In modeling the data at higher temperatures ( $T \geq 8$  K), the time-dependent depolarization curves can be fit by a stretched exponential function

$$P(t) = A_S \exp[-(\lambda_S t)^\beta], \quad (1)$$

where  $A_S$  is the asymmetry of the depolarization, normalized to the independently measured full asymmetry,  $\lambda_S$  is the slow depolarization rate and  $\beta$  is the stretched exponent. For the ISIS data,  $A_S$  and  $\lambda_S$  are both left as fit parameters, since the onset of fast depolarization will be manifest in a loss of apparent asymmetry. For the GPS data, the asymmetry was independently measured and  $A_S$  was fixed at this value. The results

are shown in Fig. 3 where above 10 K we see excellent agreement between the results taken at the two different facilities. The slow depolarization rate  $\lambda_S$  shows a clear change at 120 K, close to the temperature at which the magnetization exhibits the onset of hysteretic behavior (see inset of Fig. 3). Below 10 K, a dramatic increase in the relaxation rate is observed. For the EMU data,  $A_S$  is nearly constant near its full value at higher temperatures indicating that fast relaxation processes are negligible. However, below about 10 K,  $A_S$  drops rapidly, reaching a value of approximately 0.39(1) of the full asymmetry at 1.6 K. This behavior clearly demonstrates the onset of fast depolarization processes, and accounts for the difference in  $\lambda_S$  for the two data sets below 10 K. The exponent  $\beta$  (results not shown) for both the GPS and EMU data has a value  $1.05 \pm 0.02$  at high temperatures, drops to  $0.80 \pm 0.02$  below 120 K, then drops again below 20 K to a value of  $0.5 \pm 0.05$  at 8 K.

In Fig. 4, we show a sequence of low-temperature depolarization curves taken on GPS, where the fast relaxation processes can be observed. Upon cooling below  $T = 8$  K, we see the onset of spontaneous oscillations, unambiguously demonstrating the existence of magnetic ordering. The oscillations are heavily damped, and attempts to fit the data to the expected two-component depolarization function for polycrystalline samples with magnetic order as utilized in Ref. 9 and 10 were unsuccessful. A three-component depolarization function of the form

$$P(t) = A_1 \exp(-\lambda_1 t) \cos(\omega_\mu t + \phi) + A_2 \exp(-\lambda_2 t) + A_s \exp[-(\lambda_s t)^\beta], \quad (2)$$

yields an adequate fit to the data, as shown in Fig. 4. We find a muon precession frequency  $\omega_\mu/2\pi = 8.8(2)$  MHz, corresponding to an average local field for the precessing muons of  $\langle B_{loc} \rangle = \omega_\mu / \gamma_\mu = 665$  G, where  $\gamma_\mu$  is the muon gyromagnetic ratio and  $\gamma_\mu / 2\pi = 0.01355$  MHz/G. This value is consistent with Fourier transforms of the data, although the Fourier peak is quite broad, with a half-width of approximately 5 MHz. The extracted frequency is significantly smaller than the 13.3 MHz value observed for  $\text{Eu}_2\text{Ir}_2\text{O}_7$  ( $\langle B_{loc} \rangle_\mu = 987$  G) [9], and the 14.8 MHz ( $\langle B_{loc} \rangle_\mu = 1100$  G) found for  $\text{Y}_2\text{Ir}_2\text{O}_7$ , and  $\text{Yb}_2\text{Ir}_2\text{O}_7$  [10]. The difference in frequency is apparent when comparing the  $T = 1.8$  K depolarization curves for  $\text{Nd}_2\text{Ir}_2\text{O}_7$  and  $\text{Yb}_2\text{Ir}_2\text{O}_7$  [10], which is also shown in Fig. 4.

The depolarization rates are  $\lambda_1 = 13(1) \mu\text{s}^{-1}$ ,  $\lambda_2 = 15(2) \mu\text{s}^{-1}$ ,  $\lambda_s = 0.18(1) \mu\text{s}^{-1}$ , and  $\beta = 1.07(6)$ ; the relative amplitudes are  $A_1 = 9.3$ ,  $A_2 = 6.7(6)$ , and  $A_s = 7.1(4)$ ; the total amplitude  $A_1 + A_2 + A_s$  was constrained to be the measured full asymmetry, with the ratio of slowly decaying asymmetry to the total asymmetry,  $\eta \equiv A_s/A_1$ , found to be approximately 0.30(2). The resultant phase angle is extremely large,  $\phi = -63^\circ$  and the fit deviates from the data at very short times.

We also achieved a reasonable alternative fit of the data at 1.6 K using a two-component Bessel function:

$$P(t) = A_1 \exp(-\lambda_1 t) J_0(\omega_\mu t) + A_2 \exp(-[\lambda_2 t]^\beta), \quad (3)$$

where  $J_0$  is the spherical Bessel function of the first kind, as commonly used in systems exhibiting spin density wave ordering [15]. For Eq. 3, we extracted the parameters  $\omega_\mu/2\pi = 8.26$  MHz,  $\lambda_1 = 9.8 \mu\text{s}^{-1}$ ,  $\lambda_2 = 0.23 \mu\text{s}^{-1}$ ,  $\beta = 0.45$ , and  $\eta = 0.42$ . Although this fit captured the very short and long times accurately, it failed to accurately describe the entire time interval below 1  $\mu\text{s}$ . Nonetheless, both fits allow us to reasonably estimate the local field, and extract the rate of the slow depolarization term below 8 K (also shown in Fig. 3 for Eq. 2) Here the relative contribution of  $A_2$  of the total asymmetry as well as  $\lambda_s$  are found to be roughly independent of temperature below 5 K.

For the low temperature longitudinal field measurements conducted on EMU, the fast decaying component is not detected by the spectrometer and so at low temperatures we are only measuring the slowly relaxing component (equivalent to the third component in Eq. 2). Our results (see Supplemental Figure) at  $T = 1.6$  K for the fractional asymmetry  $\eta_S = A_s/A_{total}$  and the depolarization rate  $\lambda_S$  (via Eq. 1) have zero-field limits of  $\eta_S = 0.36(1)$  and  $\lambda_S = 0.17(2) \mu\text{s}^{-1}$ , in good agreement with the GPS results. A field of about 350 G is required to restore half of the missing asymmetry by decoupling the muon from the local magnetic field, roughly a factor two lower than the characteristic precession field of 665 G. We also find that the depolarization rate  $\lambda_S$  is independent of applied field up to 300 G, at which point the muon is decoupling from the local field. Since  $\lambda_S / \gamma_\mu \approx 2$  G, the lack of magnetic field dependence in  $\lambda_S$  demonstrates that the long-time depolarization is dynamical in origin. The temperature independence of the

depolarization rate below 5 K (Fig. 3) suggests that quantum rather than thermal fluctuations are important in this regime.

We now turn to the nature of the low-temperature ordered magnetic state. Our magnetization results strongly suggest that the ordering is on the  $\text{Ir}^{4+}$  sublattice, while the  $\text{Nd}^{3+}$  moments remain in a paramagnetic state. This ordered state is unusual, as evidenced by the highly damped oscillations and lack of detectable neutron scattering peaks associated with this order. Assuming the muon stopping site(s) are the same for all the  $\text{A}_2\text{Ir}_2\text{O}_7$  materials, the low muon precession frequency observed for  $\text{Nd}_2\text{Ir}_2\text{O}_7$  indicates that the magnetic structure is different than that for the Eu, Y, and Yb based materials. We infer from these results two different scenarios: the underlying correlations may produce a ‘small-moment’ system, as observed in  $\text{UPt}_3$  or  $\text{URu}_2\text{Si}_2$  [20], or alternatively, the magnetic order could have a small correlation length. The muon depolarization following Eq. 3, based on a Bessel function, favors the former scenario, while the three-component depolarization described by Eq. 2 combined with the potential presence of strong frustration in the system would seem to favor the latter scenario.

The onset of magnetism at 120 K, as indicated by both the magnetization and  $\mu\text{SR}$  measurements, combined with the lack of spontaneous muon precession at this temperature indicates there is no long-range ordering at this transition. In this temperature region, the system is clearly metallic, demonstrating that geometric frustration, if present, is not relieved by an MI transition, and these results are in contrast to the ordering observed at this same temperature in the insulating  $\text{Eu}_2\text{Ir}_2\text{O}_7$ ,  $\text{Y}_2\text{Ir}_2\text{O}_7$ , and  $\text{Yb}_2\text{Ir}_2\text{O}_7$  materials [9, 10]. This ordered phase may be of the spin-glass variety, and our data are also consistent with the prediction of a highly degenerate 2in/2out structure [22]. The resulting behavior is intermediate between the results reported for  $\text{Pr}_2\text{Ir}_2\text{O}_7$  (disordered metallic ground state [11, 19]) and the three insulating systems mentioned above, confirming the variation of correlations and change in the band structure with ionic radius.

Our observation of paramagnetic  $\text{Nd}^{3+}$  moments is inconsistent with the results presented in Ref. 14, where it was suggested the lowest lying crystal field doublet of the  $\text{Nd}^{3+}$  ion is split below  $T = 15$  K, below the M-I transition at  $T_{MI} = 37$  K. Indeed, it is not clear from our data that any MI transition occurs in this system, as evidenced by the

tendency towards a saturation of the resistivity versus temperature at low temperatures. Also, the variation of the magnetoresistance  $\Delta\rho=\rho(H)/\rho(0)-1$  with magnetization is *negative* and varies linearly with  $M^2$  (inset, Fig 4), analogous to the Kondo screening observed in  $\text{Pr}_2\text{Ir}_2\text{O}_7$ , where both the RKKY interaction strength and Kondo temperature are approximately 20 K [19]. At ambient pressure, no magnetoresistance has been reported in  $\text{A}_2\text{Ir}_2\text{O}_7$  with a nonmagnetic A-site; however removing the MI transition of  $\text{Eu}_2\text{Ir}_2\text{O}_7$  through the application of high pressure [21] showed that this material exhibits positive magnetoresistance proportional to  $H^2$ , similar to normal metals. We assert that an additional magnetic scattering channel must be present in  $\text{Nd}_2\text{Ir}_2\text{O}_7$ , and it is this process, rather than a MI transition that causes the upturn in the resistivity of  $\text{Nd}_2\text{Ir}_2\text{O}_7$  below 8K. We propose that  $\text{Nd}_2\text{Ir}_2\text{O}_7$  exhibits behavior intermediate between the magnetically ordered insulating and the non-ordered metallic iridate pyrochlores: it is weakly metallic, with magnetic order facilitated by the RKKY interaction.

In summary, we have studied high quality  $\text{Nd}_2\text{Ir}_2\text{O}_7$  samples via magnetization, resistivity, and  $\mu\text{SR}$ . We find the onset of disordered magnetism at  $T = 120$  K, likely arising from the geometric frustration of the  $\text{Ir}^{4+}$  sublattice. Below  $T = 8$  K, magnetic order appears albeit heavily damped. We find no evidence for a metal-insulator transition, suggesting that the magnetic ordering is facilitated by an RKKY interaction. More detailed studies via both  $\mu\text{SR}$  and neutron scattering are required to understand the structure of the magnetically ordered state, its relationship to a metal-insulator transition, and the implications regarding the existence of possible novel ground states such as the Weyl semi-metal [4].

This work was supported in part by National Science Foundation Materials World Network grant DMR-0710525 and by NSF CAREER award DMR-1056625. Muon experiments were performed at the ISIS Muon Facility at the Rutherford Appleton Laboratories (UK) and the Swiss Muon Source at the Paul Scherrer Institute (Switzerland). Part of this work was performed at Oak Ridge National Laboratory High Flux Isotope Reactor, sponsored by the Scientific User Facilities Division, Office of Basic Energy Sciences, U.S. Department of Energy.

## References

- [1] J. S. Gardner, M. J. P. Gingras, and J. E. Greedan, *Rev. Mod. Phys.* **82**, 53 (2010).
- [2] M. J. Harris, S. T. Bramwell, D. F. McMorrow, Th. Zeiske, and K. W. Godfrey, *Phys. Rev. Lett.* **79**, 2554 (1997).
- [3] D. Pesin and L. Balents, *Nature Physics* **6**, 376 (2010).
- [4] X. Wan, A. M. Turner, A. Vishwanath, and S. Y. Savrasov, *Phys. Rev. B* **83**, 205101 (2011).
- [5] D. Yanagishima and Y. Maeno, *J. Phys. Soc. Jpn.* **70**, 2880 (2001).
- [6] N. Taira, M. Wakeshima, and Y. Hinatsu, *J. Phys. Cond. Matt.* **13**, 5527 (2001).
- [7] K. Matsuhira, M. Wakeshima, R. Nakanishi, T. Yamada, A. Nakamura, W. Kawano, S. Takagi, and Y. Hinatsu, *J. Phys. Soc. Jpn.* **76**, 043706 (2007).
- [8] Y. Machida, S. Nakatsuji, Y. Maeno, T. Tayama, T. Sakakibara, and S. Onoda, *Phys. Rev. Lett.* **98**, 057203 (2007).
- [9] S. Zhao, J. M. Mackie, D. E. MacLaughlin, O. O. Bernal, J. J. Ishikawa, Y. Ohta, and S. Nakatsuji, *Phys. Rev. B* **83**, 180402(R) (2011).
- [10] S. M. Disseler, C. Dhital, T. C. Hogan, A. Amato, C. Baines, S. Giblin, S. D. Wilson, and M. J. Graf, manuscript in preparation (2011).
- [11] D. E. MacLaughlin, Y. Ohta, Y. Machida, S. Nakatsuji, G. M. Luke, K. Ishida, R. H. Heffner, Lei Shu, and O. O. Bernal, *Physica B* **404**, 667 (2008).
- [12] M. Sakata, T. Kagayama, K. Shimizu, K. Matsuhira, S. Takagi, M. Wakeshima, and Y. Hinatsu, *Phys. Rev. B* **83**, 041102(R) (2011).
- [13] U. Walter, *J. Phys. Chem Solids* **4**, 401 (1984)
- [14] K. Tomiyasu, K. Matsuhira, K. Iwasa, M. Watahiki, S. Takagi, M. Wakeshima, Y. Hinatsu, M. Yokoyama, K. Ohoyama, and K. Yamada, arXiv:1110.6605 (2011).
- [15] See A. Amato, *Rev. Mod. Phys.* **69**, 1119 (1997), or for a more detailed review, *Muon Spin Rotation, Relaxation, and Resonance : Applications to Condensed Matter*, A. Yaouanc and P. Dalmas de Réotier, (Oxford University Press, Oxford, 2011).
- [16] A. Olariu, P. Mendels, F. Bert, B. G. Ueland, P. Schiffer, R. F. Berger, and R. J. Cava, *Phys. Rev. Lett.* **97**, 167203 (2006).
- [17] A. Koda, R. Kadono, K. Ohishi, S. R. Saha, W. Higemoto, S. Yonezawa, Y. Muraoka, and Z. Hiroi, *J. Phys. Soc. Jpn.* **76**, 063703 (2007).

- [18] N. Taira, M. Wakeshima, Y. Hinatsu, A. Tobo, and K. Ohoyama, *J. Solid State Chem.* **76**, 165 (2003).
- [19] S. Nakatsuji, Y. Machida, Y. Maeno, T. Tayama, T. Sakakibara, J. van Duijn, L. Balicas, J. N. Millican, R. T. Macaluso, and J. Y. Chan, *Phys. Rev. Lett.* **95**, 087204 (2006), and references therein.
- [20] A. Amato, M. J. Graf, A. de Visser, H. Amitsuka, D. Andreica, and A. Schenck, *J. Phys.: Condens. Matter* **16**, S4403 (2004).
- [21] F. F. Tafti, J. J. Ishikawa, A. McCollam, S. Nakatsuji, and S. R. Julian, arXiv 1107.2544v1
- [22] A. Ikeda, H. Kawamura *J. Phys. Soc. Jpn.* **77**, 073707 (2008).

## Figure Captions

Figure 1. (a) Magnetization versus temperature in an applied field of 1000 G for field cooled (solid symbols) and zero field cooled (open symbols) sample of  $\text{Nd}_2\text{Ir}_2\text{O}_7$ . Inset: Expanded view of the susceptibility in the vicinity of  $T = 120$  K. (b) Resistivity versus temperature for  $\text{Nd}_2\text{Ir}_2\text{O}_7$  in applied fields of 0 T, 4 T, and 9 T.

Figure 2. Magnetic field dependence of the resistivity and magnetization at  $T = 1.8$  K. The dashed line shows the fit to a Brillouin function as described in the text. Inset: variation of the fractional change in resistivity with the square of the magnetization, with magnetic field as an implicit parameter; the straight line is a guide to the eye.

Figure 3. Temperature dependent muon depolarization rate for extracted from data taken at ISIS and PSI, as described in the text. Inset: Expanded view of the depolarization rate in the vicinity of  $T = 120$  K. Solid lines are guides to the eye.

Figure 4. Evolution of the short-time muon depolarization curves (PSI) with decreasing temperature. The upper four curves are for  $\text{Nd}_2\text{Ir}_2\text{O}_7$ , at temperatures of 8 K, 5 K, 3.5 K, and 1.6 K from top to bottom. The bottom curve is for  $\text{Yb}_2\text{Ir}_2\text{O}_7$  at 1.6 K (from Ref. 10). Curves are offset for clarity. The solid lines are fits to Eq. 1 for the  $T = 8$  K data and to Eq. 2 for the  $T = 1.6$  K data.

Supplemental Figure. Longitudinal magnetic field dependence of the depolarization rate and fractional asymmetry component at  $T = 1.6$  K extracted from data taken at ISIS.

Figure 1

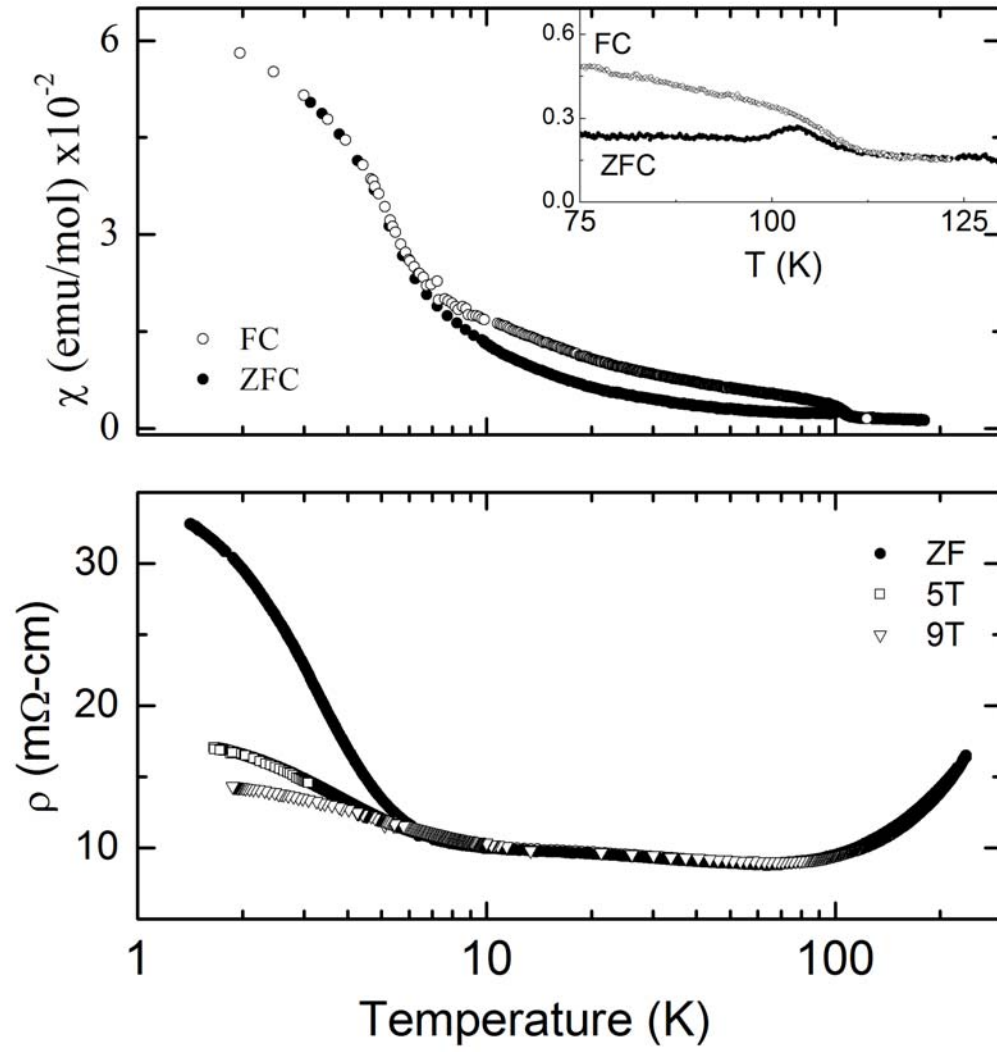


Figure 2

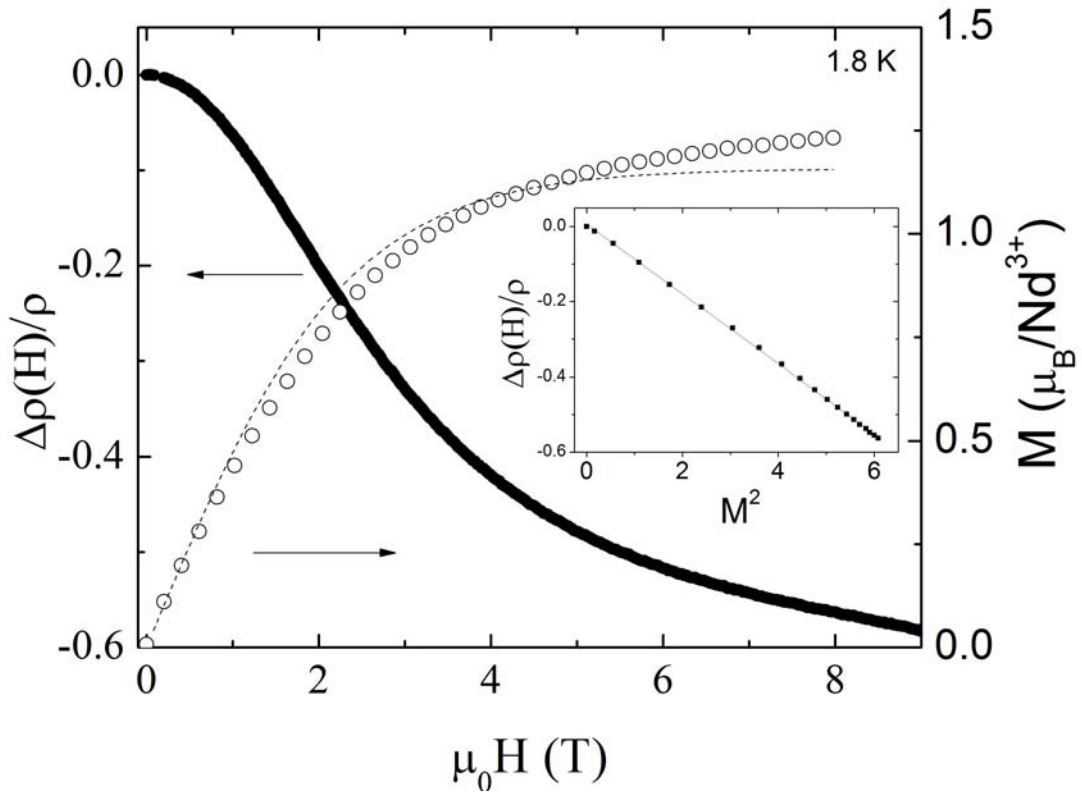


Figure 3

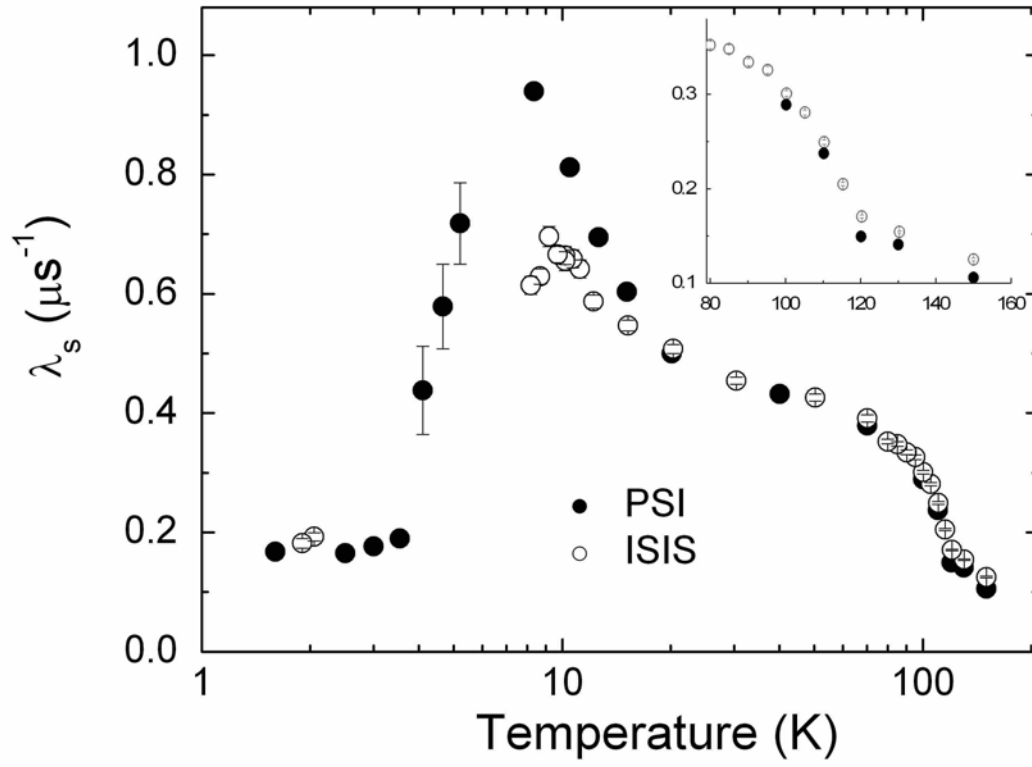
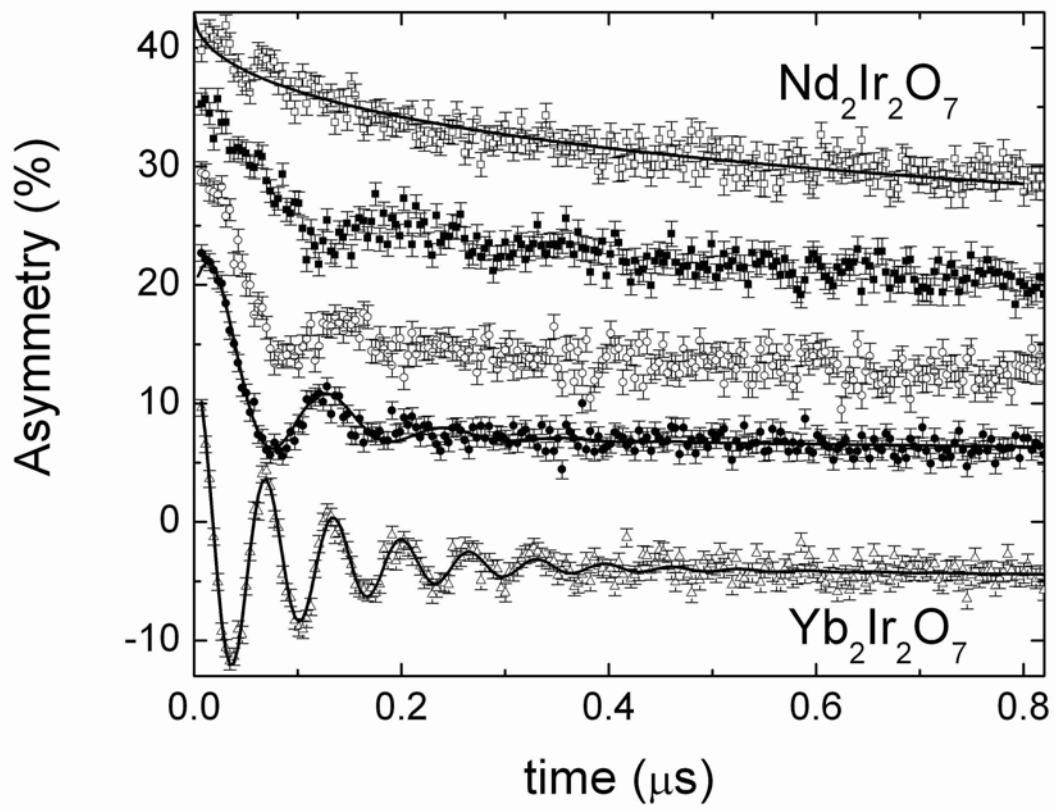


Figure 4



Supplemental Figure

